ISSN 1936-878X/09/$36.00
PUBLISHED BY ELSEVIER INC.
DOI:10.1016/j.jcmg.2009.04.012

Specific Targeting of Human Inflamed Endothelium and In Situ Vascular Tissue Transfection by the Use of Ultrasound Contrast Agents

Olga Barreiro, PHD,*† Río J. Aguilar, MD, PHD,‡ Emilio Tejera, PHD,*†
Diego Megías, PHD,§ Fernando de Torres-Alba, MD,‡ Arturo Evangelista, MD, PHD,‡
Francisco Sánchez-Madrid, PHD*†

Madrid and Barcelona, Spain

OBJECTIVES We used human umbilical cord segments as an ex vivo model to investigate the possible clinical diagnostic and therapeutic applications of microbubbles (MBs).

BACKGROUND Microbubbles are commonly used in clinical practice as ultrasound contrast agents. Several studies have addressed the in vivo applications of MBs for specific targeting of vascular dysfunction or sonoporation in animal models, but to date no human tissue model has been established.

METHODS Primary venular endothelial cell monolayers were targeted with MBs conjugated to an antibody against a highly expressed endothelial marker (tetraspanin CD9), and binding was assessed under increasing flow rates (0.5 to 5 dynes/cm^2). Furthermore, CD9-coupled MB endothelial targeting was measured under flow conditions by contrast-enhanced ultrasound analysis in an ex vivo human macrovascular model (umbilical cord vein), and the same tissue model was used for the detection of inflamed vasculature with anti-intercellular adhesion molecule (ICAM)-1–coated MBs. Finally, plasmids encoding fluorescent proteins were sonoporated into umbilical cord vessels.

RESULTS Specific endothelial targeting in the in vitro and ex vivo models described previously was achieved by the use of MBs covered with an anti-CD9. Furthermore, we managed to induce inflammation in umbilical cord veins and detect it with real-time echography imaging using anti–ICAM-1–coupled MBs. Moreover, expression and correct localization of green fluorescent protein and green fluorescent protein-tagged ICAM-1 were assessed in this human ex vivo model without causing vascular damage.

CONCLUSIONS In the absence of clinical trials to test the benefits and possible applications of ultrasound contrast agents for molecular imaging and therapy, we have developed a novel ex vivo human model using umbilical cords that is valid for the detection of inflammation and for exogenous expression of proteins by sonoporation. (J Am Coll Cardiol Img 2009;2:997–1005) © 2009 by the American College of Cardiology Foundation

From the *Servicio de Inmunología, Hospital de la Princesa, Universidad Autónoma de Madrid, Madrid, Spain; †Departamento de Biología Vascular e Inflamación, Centro Nacional de Investigaciones Cardiovasculares, Madrid, Spain; ‡Servicio de Cardiología, Hospital Vall d'Hebron, Barcelona, Spain; and §Unidad de Microscopía, Centro Nacional de Investigaciones Oncológicas, Madrid, Spain. This work was supported by Salud SAF 2008-02635, Red Temática de Investigación Cooperativa en Enfermedades Cardiovasculares grant RD06/0014-0030 to Dr. Sánchez-Madrid, EU grant LSHG-CT-2003-502935 to Dr. Barreiro, and "Ayuda a la Investigación Básica 2007 Sociedad Española de Cardiología" to Dr. Aguilar. The CNIC is supported by the Spanish Ministry of Health and Consumer Affairs and the Pro-CNIC Foundation. Drs. Barreiro and Aguilar contributed equally to this work.

Manuscript received December 12, 2008; revised manuscript received April 9, 2009, accepted April 29, 2009.

Microbubbles (MBs) are 2- to 8-μm acoustically active particles consisting of a gaseous core surrounded by a biocompatible shell typically composed of a mix of lipids, albumin, or polymers. The resonant properties of MB make them a powerful class of ultrasound contrast agents with both diagnostic and therapeutic applications. In this regard, MBs can be modified by the conjugation to their shell of specific ligands, such as peptides or monoclonal antibodies, to create site-targeted MBs able to detect molecular changes in endothelium (e.g., inflammation, thrombosis, angiogenesis) (1). Insonation of MBs can produce transitory micropores at cell membranes (2), offering the possibility of delivering bioactive substances or genetic material into surrounding cells, a procedure termed sonoporation (3).

See page 1006

ABBREVIATIONS AND ACRONYMS

EGFP = enhanced green fluorescent protein

HUVEC = human umbilical vein endothelial cell

ICAM = intercellular adhesion molecule

MB = microbubble

TNF = tumor necrosis factor

US = ultrasound

To date there have been several reports of ultrasound (US) imaging of MBs and sonoporation in human vascular monolayers cultured in vitro (4,5). Using a human ex vivo model based on umbilical cord segments, we evaluated real-time US molecular imaging of MBs targeted either to a general endothelial surface receptor (CD9) or a marker of inflamed endothelium (intercellular adhesion molecule [ICAM]-1) and assessed the feasibility of sonoporation for the delivery of functional plasmids to the endothelium of a human vessel.

METHODS

Microbubble preparation. Biotinylated lipid-encapsulated perfluorocarbon MBs were purchased (Targeson LLC, Charlottesville, Virginia). Microbubbles were prepared following manufacturer's instructions at a final concentration of 4 to 5 $\times$ 10^6 MBs per milliliter in saline solution, as determined with a hemocytometer XT-1800i (SYSMEX, Mundelein, Illinois). Alternatively, a vial of SonoVue (Bracco International B.V., Amsterdam, the Netherlands) was resuspended following the manufacturer's instructions (8 μl of sulphur hexafluoride per milliliter).

Ultrasound image acquisition from umbilical cord segments. The veins of umbilical cord segments were cannulated and washed with a heparinated solution (20 UI/ml). Paired segments from the same cord were treated as follows: one was filled with 199 medium containing growth factors and the other with medium with 100 ng/ml tumor necrosis factor (TNF)-α to induce inflammatory conditions. Both segments were incubated 20 h at 37°C and were then immersed in a saline bath at 37°C for MB perfusion using an automated infusion syringe pump (VueJect [BR-INF 100, Bracco Research SA, Geneva, Switzerland]) and image acquisition. Segments were scanned with a Vivid i digital cardiovascular ultra-portable ultrasound system (GE Healthcare, Milwaukee, Wisconsin) with an i12LR high-frequency linear transducer (up to 13 MHz, using 4.5 to 9.9 MHz with second harmonic). Solutions of MB (2 to 5 million MB per milliliter in a total volume of 10 ml) were perfused using a pump at 1.6 ml/min. Video sequences were stored and subsequently analyzed with EchoPac 6.3 software (GE Healthcare).

Sonoporation of endothelium in intact human umbilical cord blood vessels. For sonoporation, the Vivid i digital ultrasound system with a different transducer (S3 multifrequency) (GE Healthcare) was used. A solution of SonoVue mixed with 20 μg/ml plasmid deoxyribonucleic acid (DNA) was introduced into the lumen of umbilical arteries, and the vessels were tied off at both ends. Insonation was performed at harmonic imaging (1.7 to 3.4 MHz) at a high frame rate (112 Hz) and at a high mechanical index (1.3) for ~5 min. After insonation, artery segments were maintained for 20 h in growth factor supplemented medium 199, fixed in 4% paraformaldehyde, and processed for tissue microscopy analysis. In the case of umbilical vein experiments, 10 ml of the same mixture of MB and complementary DNA were perfused with a VueJect pump (Bracco Imaging, Milan, Italy) at a rate of 1.6 ml/min across human endothelial veins with simultaneous insonation that used the same frequency and mechanical index but a frame rate between 25 and 35 Hz. Then, endothelial cells were isolated from the vein (6) immediately after insonation and cultured for 20 h before being fixed in 4% paraformaldehyde and prepared for cellular microscopy analysis (Online Appendix). Institutional Review Board approval for the studies was obtained from the National Center of Cardiovascular Research and Hospital Universitario de la Princesa (IRB00005840).

RESULTS

Microbubble-mediated specific targeting under controlled physiological shear flow. To evaluate specific targeting of human vascular tissues with US contrast agents (MB), we first analyzed the ability of antibody-directed MBs to bind endothelial surfaces under flow

conditions. Monolayers of primary human umbilical vein endothelial cells (HUVECs) were either left under resting conditions or were activated with the proinflammatory cytokine TNF-α and then mounted in an inverted parallel flow chamber for MB attachment evaluation by optical microscopy.

To test specific endothelial targeting, biotinylated Targestar^{B} MBs were coupled to an antibody against CD9 (a cell-surface protein highly expressed in HUVECs) (Fig. 1A) (7). For controls, we used naked (nonantibody-coupled) biotinylated MB and biotinylated MB coupled to an isotype-matched antibody raised against the adhesion molecule ICAM-3 (whose expression is hardly detectable in HUVECs) (Fig. 1A). The MBs were drawn across the HUVECs at increasing flow rates, and the numbers of attached MB at each flow rate were counted and compared between different treatments (Figs. 1B and 1C). Nonspecific binding was assessed by the binding of MBs to plates coated with the substratum used for HUVEC cultures (fibronectin) and was very low in all cases.

We found that MBs coated with anti-CD9 (anti-CD9-MB) bound strongly to resting and activated HUVEC monolayers, showing up to 9-fold greater binding than controls. The exponential phase of binding lasted up to 2 dynes/cm^2. The MB binding was impaired by the increasing shear stress at high flow rates; however, there was no significant detachment during the experiment and the subsequent washout, indicating strong attachment. Isotype-control MBs and naked MBs showed some residual nonspecific binding that decreases with the increase of flow rate (Fig. 1B).

Real-time echography imaging of MB-mediated vascular targeting in ex vivo human umbilical cord veins. Having validated endothelial targeting of MB in the in vitro flow chamber, we next evaluated vascular MB targeting in an ex vivo model of human macrovascular tissue, the umbilical cord vein. Umbilical veins in cord segments were perfused with anti–CD9-MB, and images were collected throughout the experiment until after the last washout. We found that MB remained acoustically active after conjugation with antibody, and individual MBs attached to the vein wall were even detected with submillimetric resolution. During the washout period, the umbilical vein was fully coated with MB, delineating the vein wall. To rule out nonspecific adhesion, parallel control experiments were conducted with the ICAM-3–targeted and naked MBs; no significant attachment of MB was detected in either case (Fig. 2A). Quantitative analysis of contrast-enhanced US video intensity clearly demonstrated the specificity of anti–CD9-MB binding compared with the residual adsorptive attachment of control antibody-coupled or naked MB (Figs. 2B and 2C).

Detection of inflamed endothelium by MB-mediated targeting. CD9 is constitutively expressed in endothelial cells, and its membrane expression is not significantly altered by proinflammatory stimulation (7). Accordingly, treatment of umbilical cord veins with proinflammatory stimuli (TNF-α) produced no change in the specific targeting of anti–CD9-MB (data not shown). To specifically target inflamed vascular beds, we conjugated MBs to an antibody against the adhesion molecule ICAM-1, which is up-regulated during inflammation. The effectiveness of the inflammatory activation was confirmed by isolating HUVECs from TNF-α–treated umbilical veins and determining the platelet/endothelial cell adhesion molecule (PECAM)-1/(CD31)–ICAM-1/(CD54) double-positive population by fluorescence-activated cell sorting; cell-surface expression of ICAM-1 after TNF-α treatment was increased 2-fold with respect to resting conditions (Fig. 3A). Ultrasound imaging of ICAM-1–targeted MB barely detected basal ICAM-1 expression in resting umbilical cords, whereas a 10-fold increase in MB binding was observed in inflamed tissue, demonstrating the ability of the technique to identify sites of local inflammation in the macrovasculature (Fig. 3B).

Analysis of tissue integrity after US insonation at high mechanical index. To achieve efficient in situ transfection of DNA plasmids directly into intact endothelium, we attempted to induce transitory micropores in the luminal endothelial membrane of umbilical vessels by destroying MBs with sustained high-power insonation (mechanical index: 1.2 to 1.4). Before proceeding with transfection, we first assessed the effect of the insonation on tissue integrity by immunohistochemical analysis. Hematoxylin and eosin staining revealed no apparent tissue deterioration with US insonation (Fig. 4A). Immunostaining of CD31/PECAM-1 and 4',6-diamidino-2-phenylindole (DAPI) staining for nuclei confirmed that the integrity of the monolayer seemed to be preserved (Fig. 4B). To test for possible changes in paracellular permeability, umbilical cord segments were incubated after insonation with fluorescein isothiocyanate (FITC)/dextran (77 kDa). Microscopy analysis of cryostat sections revealed an increase in paracellular permeability in US-treated cord samples compared with noninsonated cord samples. This increase was not significantly greater than that induced by our standard inflammatory treatment with TNF-α (Fig. 4C).

Sonoporation of plasmid DNA in human umbilical cord veins and arteries. Having established that US application at high mechanical index does not produce

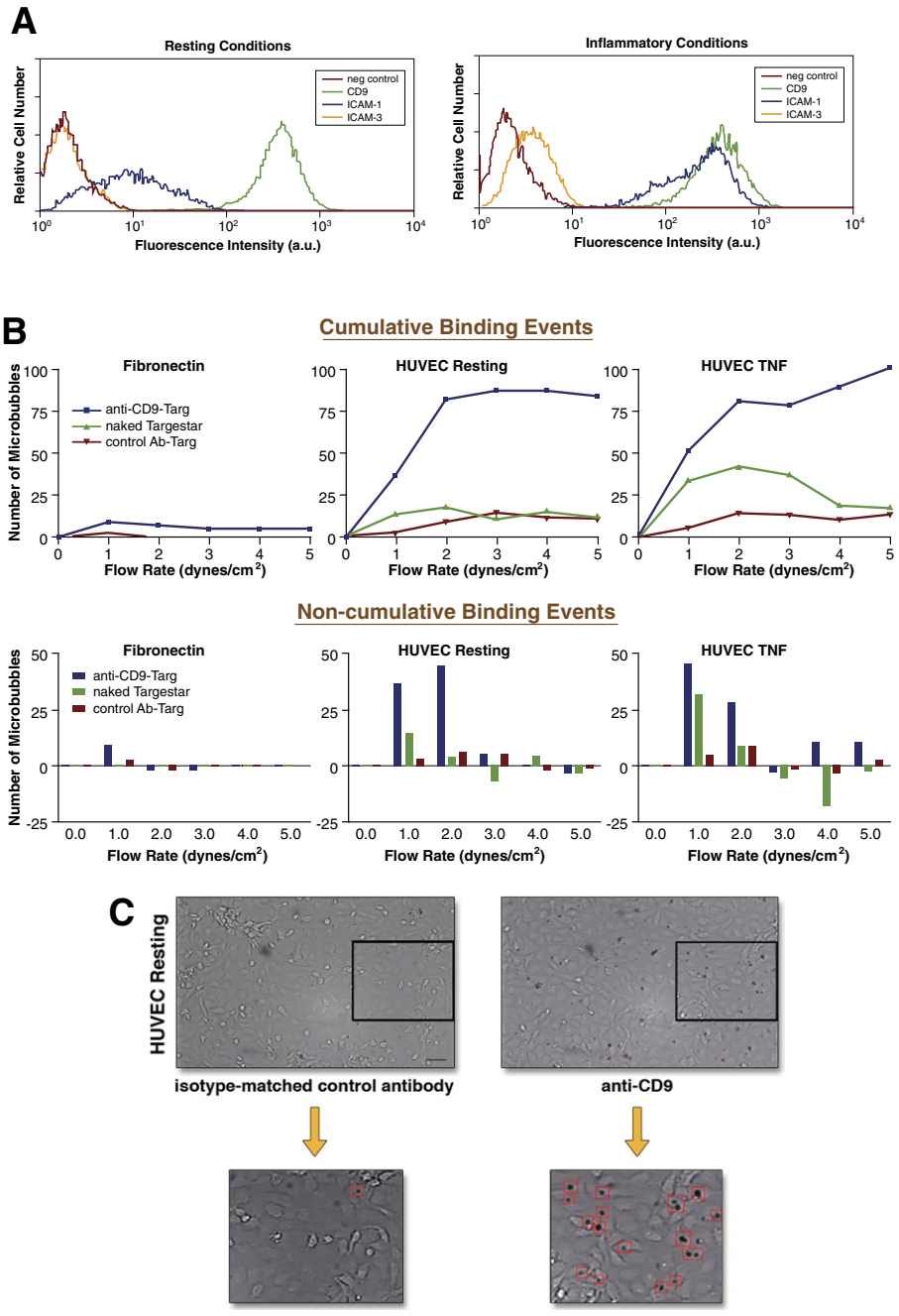

Figure 1. Study of Microbubble Specific Targeting Using a Parallel Plate Flow Chamber

(A) Flow cytometry analysis of CD9 **(green)** and intercellular adhesion molecule (ICAM)-3 **(orange)** expression in resting and tumor necrosis factor-α–activated human umbilical vein endothelial cells (HUVECs). Inducible ICAM-1 expression **(blue)** was used as positive control of tumor necrosis factor-α–induced HUVEC activation, and X-63 (**red**) was used as negative control. **(B)** Time course of attachment of Targestar^B microbubbles under flow conditions. Noncoupled biotinylated microbubbles (naked Targestar^B, **green**), microbubbles coupled to anti-CD9 **(blue)**, or to an isotype-matched ICAM-3 control antibody **(red)** were perfused at increasing flow rates over fibronectin, resting or activated HUVEC monolayers. Microbubble attachment to each substrate was quantified over time and represented in 2 different types of histograms (cumulative or noncumulative binding events). **(C)** Representative images of control versus anti–CD9-coupled microbubbles attached to resting HUVEC monolayers during the post-treatment washout period. **Boxed areas** are shown at high magnification in the **lower panels**. Microbubbles attached to the endothelial monolayers are marked with a **red outline**; those out of the focal plane were considered as not interacting with the endothelium. Screen area = 0.06 mm^2. TNF = tumor necrosis factor.

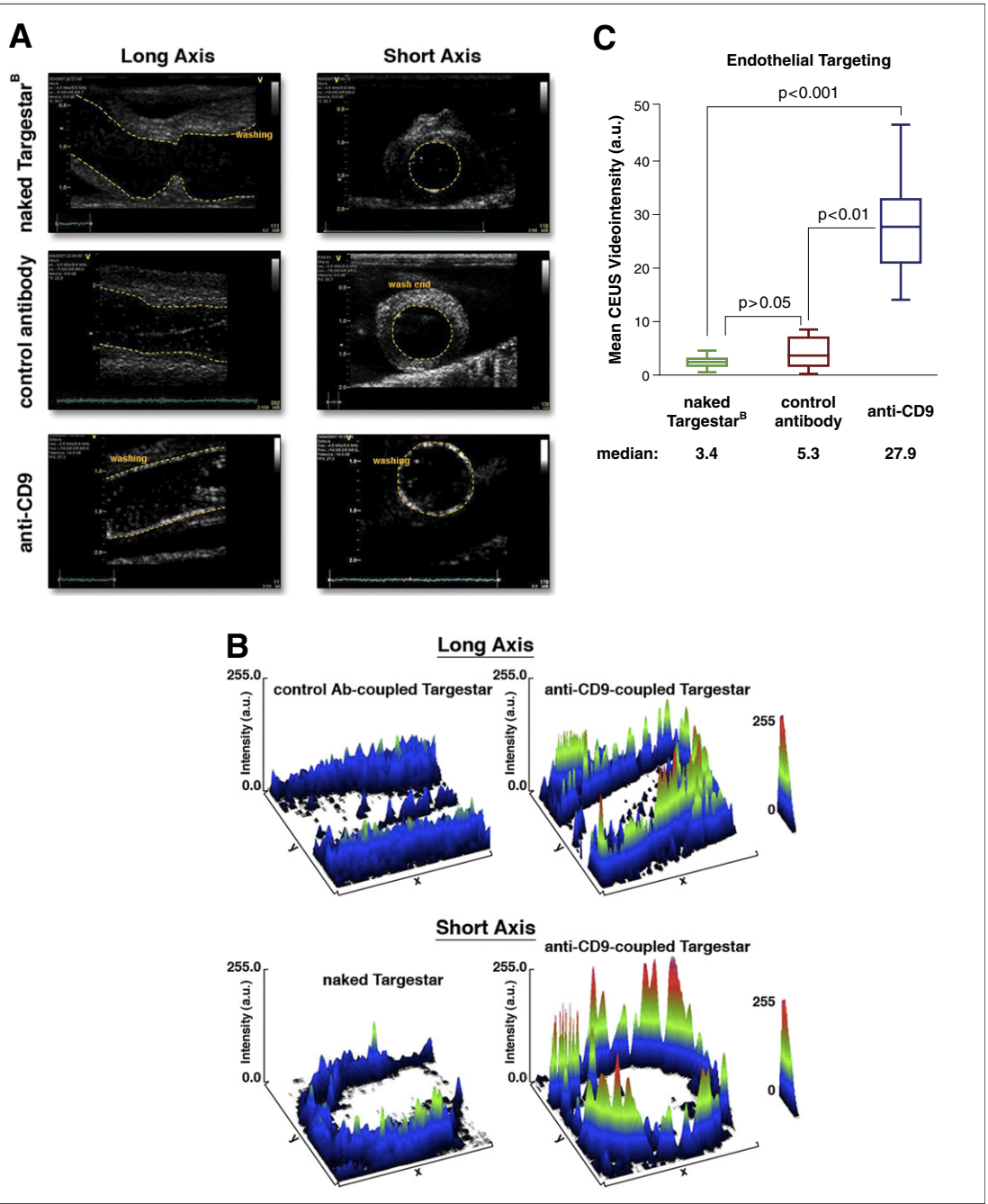

Figure 2. Echographic Analysis of Microbubble-Specific Targeting in Human Umbilical Cords

(A) Representative echographic images of the long and short axes of human umbilical cords perfused with naked, control antibody-, or anti–CD9-coupled Targestar^B microbubbles. Images are of umbilical cords maintained under resting or tumor necrosis factor-α inflammatory conditions. **Dashed yellow lines** delineate the luminal area to distinguish the MB attached to endothelium from free-flowing ones. **(B)** Representative isosurface plots of negative **(left)** and positive **(right)** targeting images from long **(top)** and short axes **(bottom)**. **(C)** In the **box and whisker plots**, the box extends from the 25th percentile to the 75th percentile, with a line at the median (the 50th percentile). The **whiskers** extend above and below the box to show the highest and lowest values of contrast-enhanced ultrasound video intensity measured in echographic images from every treatment (n ranging from 10 to 18). Statistical analysis was performed with a Kruskal-Wallis test ($p < 0.0001$) with Dunn's multiple comparison post-test (p values for all pairs of columns shown in the figure).

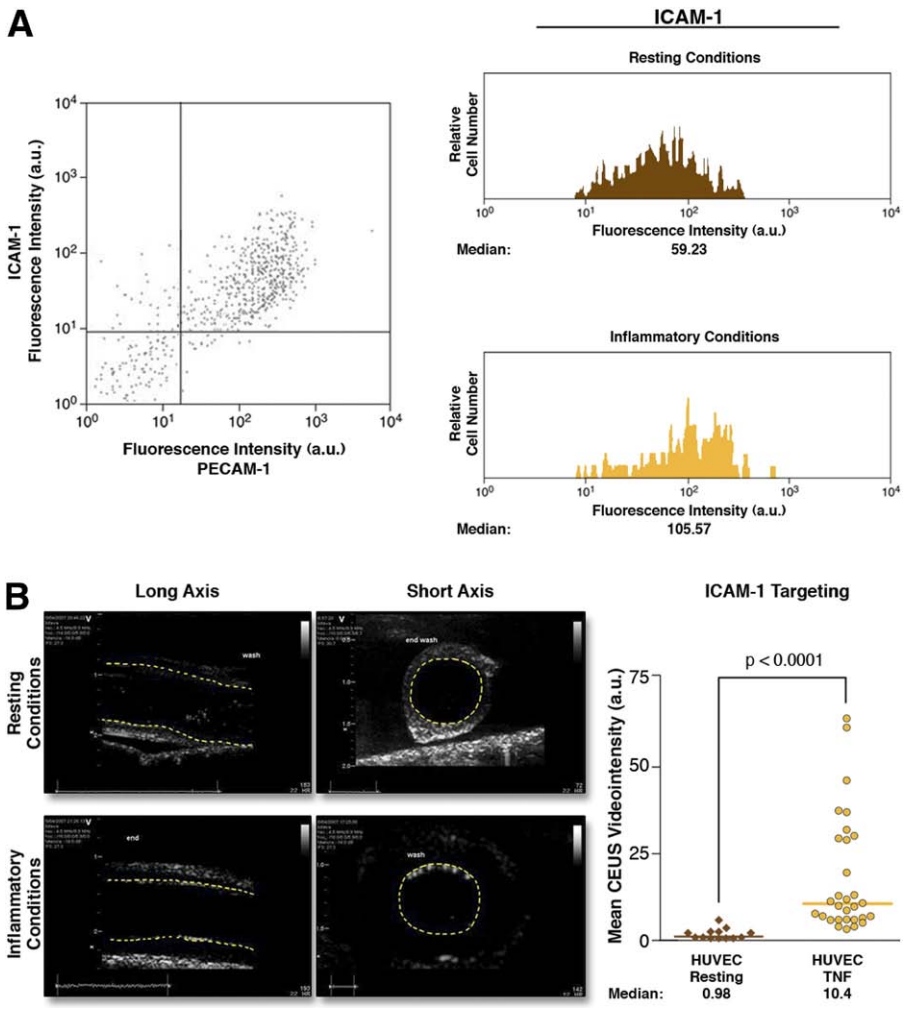

Figure 3. Echographic Detection of Inflammation by Specific Microbubble Targeting

(A) Umbilical cords were treated with either resting or inflammatory conditions for 16 to 20 h, then endothelial cells were isolated by collagenase P treatment, and expression of ICAM-1 in PECAM-1$^+$ (endothelial) cells was analyzed by flow cytometry. **(B)** Representative echographic images from long and short axes of human umbilical cords treated with resting or inflammatory conditions and perfused with anti–ICAM-1–coupled Targestar^B microbubbles. **Dashed yellow lines** delineate the luminal area to distinguish the microbubbles attached to endothelium from free-flowing ones. The scatter plot shows contrast-enhanced ultrasound video intensity values measured in images from both treatments. Statistical analysis was performed using an unpaired *t* test with Welch's correction (p value shown in the figure).

gross denudation of the endothelium, we evaluated the method for in situ sonoporation of complementary DNA plasmids. We first confirmed US-mediated MB destruction by optical microscopy or ultrasound imaging (data not shown). For sonoporation, a mixture of SonoVue MB and plasmid DNA encoding enhanced green fluorescent protein (EGFP) was included in the lumen of umbilical arteries and incubated under static conditions with simultaneous insonation. Confocal fluorescence analysis of arterial tissue revealed in situ EGFP expression in the endothelium 24 h after sonoporation (Fig. 5A). Moreover, a mixture of SonoVue MB and ICAM-1–EGFP plasmid was perfused across umbilical veins with simultaneous insonation. Then, cells were isolated and cultured in vitro 24 h before microscopy analysis. In this way, we further confirm that delivered genes were correctly expressed because ICAM-1–EGFP was appropriately localized at the HUVEC plasma membrane, concentrated in microclusters and staining marginal microvilli (Fig. 5B).

DISCUSSION

The combination of US application with the administration of targeted MB is an attractive and well-

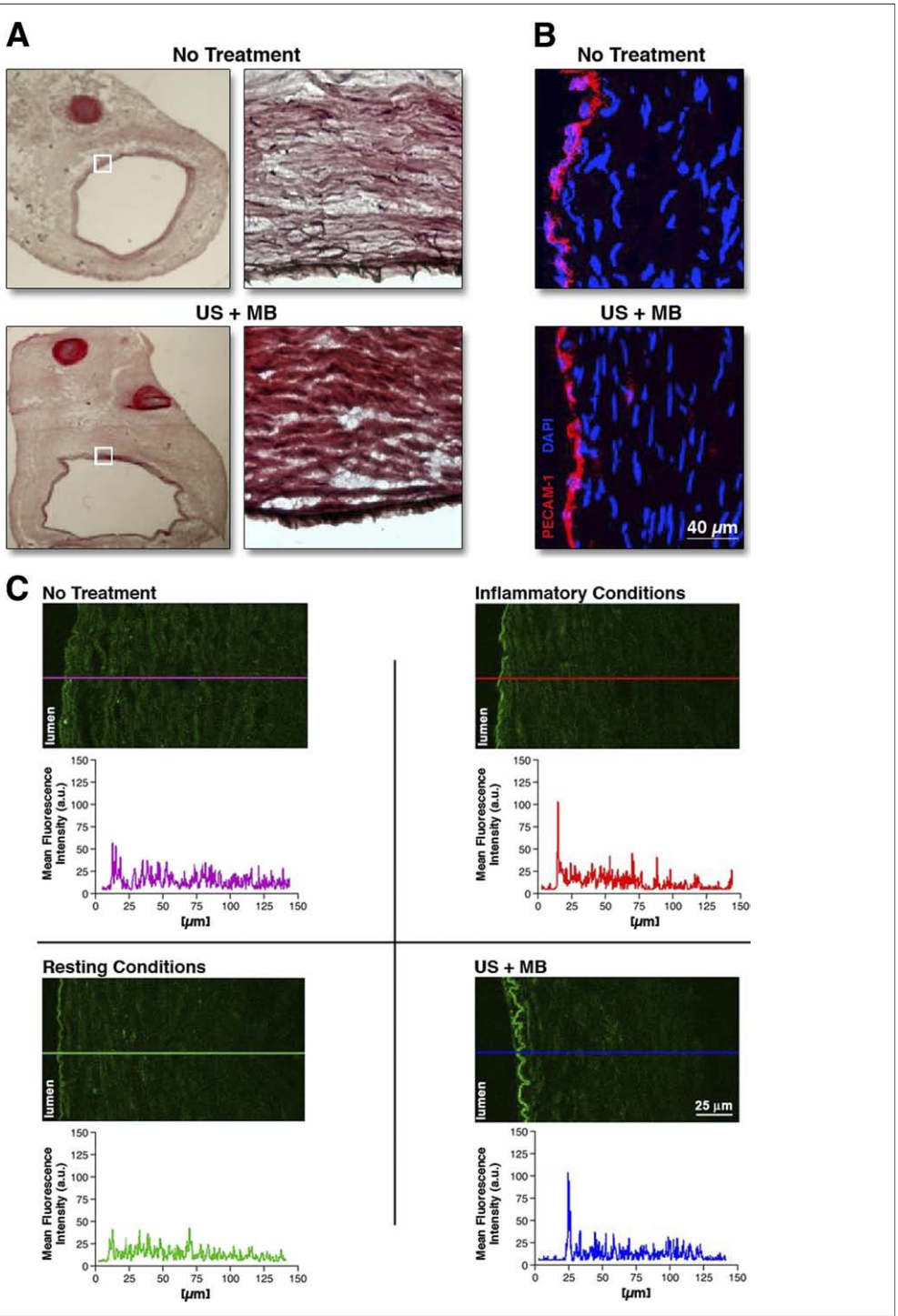

Figure 4. Study of Endothelial Viability After High Mechanical Index Ultrasound Treatment

(A) Hematoxylin and eosin staining of tissue slices from umbilical cords exposed to no treatment or to high mechanical index ultrasounds. Images on the left are full cross sections of the umbilical cords. The **white boxed areas** on them are shown at greater magnification to the right. Histology experiments were performed on 3 to 4 different cord segments for each condition, and 2 to 3 sections were analyzed from each segment **(B)** Immunostaining of tissue slices from umbilical cords shown in **(A)**. Endothelial cells were stained with an specific marker (CD31) in red and nuclei were stained with DAPI. Bar = 40 μm. **(C)** Effect of high mechanical index ultrasound on vessel wall integrity. Umbilical cords were subjected as indicated to resting or inflammatory conditions for 20 h or, alternatively, filled with a SonoVue MB solution and treated with high mechanical index ultrasounds for 5 min (US + MB) or left untreated (no treatment). Cords were perfused with fluorescein isothiocyanate (FITC)/dextran, and samples processed for fluorescence microscopy analysis. The histograms show fluorescence intensity along the line depicted on the corresponding image. All images were acquired by confocal microscopy using the same photomultiplier parameters. Bar = 25 μm.

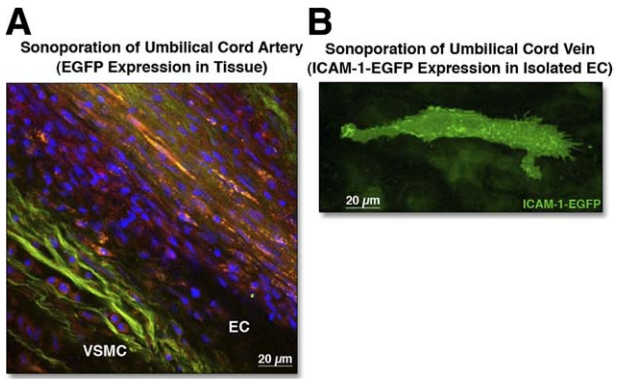

Figure 5. Sonoporation of Umbilical Cord Artery and Vein

(A) Analysis of the tissue expression of enhanced green fluorescent protein after sonoporation of an umbilical cord artery at high mechanical index. 4′,6-diamidino-2-phenylindole (DAPI) staining of nuclei **(blue)** was used to distinguish endothelial cells (EC) from muscle cells because the appearance of their nuclei reflects the orthogonal orientation of these cell types. **Green signal** corresponds to elastin autofluorescence in the vascular smooth muscle cell (VSMC) area, and **orange signal** corresponds to pseudocolored enhanced green fluorescenct protein (EGFP) after image analysis with Spectral Dye Separation tool by Leica Confocal Software. **(B)** Image showing the localization of intercellular adhesion molecule-1-enhanced green fluorescent protein at the plasma membrane of an endothelial cell grown ex vivo after high mechanical index sonoporation of a SonoVue-loaded umbilical cord vein. Bar = 20 μm.

balanced technique for both in vitro and in vivo use because of its noninvasive nature, its wide availability and relatively low cost, and its high spatiotemporal resolution, which provides sensitivity to low concentrations of targeted MB with a signal-to-noise ratio suitable for clinical use. Endothelial targeting offers great possibilities for detecting dysfunctional endothelium in atherosclerosis, vulnerable plaques, and processes associated with myocardial dysfunction such as ischemia/reperfusion or transplant rejection (8,9). Ultrasound contrast agents coupled to antibodies directed against specific vascular markers have been successfully applied in animal models during the last decade (10,11) to monitor endothelial damage or dysfunction (12), inflammation (13), angiogenesis (14), and thrombosis (15). However, no study on human tissue has been reported previously.

To evaluate endothelial targeting with MB in intact human tissue, we performed experiments on the human umbilical cord vein and artery. The human umbilical vein is a good example of macrovasculature, having a similar caliber (5 to 8 mm) to other medium-sized vessels such as the renal artery or saphenous vein. The efficiency of MB targeting for a given concentration is probably lower in macrovessels than in smaller vascular beds because the likelihood of interaction with the vessel wall for each individual MB is much reduced. For this reason, we selected CD9 tetraspanin, a molecule that is a highly expressed marker in macrovasculature and microvasculature (16), as well as in lymphatics (17), and we succeeded in detecting the entire luminal surface of the umbilical vein. CD9 plays an essential role in cell adhesion, proliferation and migration, platelet aggregation, and tumor metastasis (18). Our group has also described a regulatory role for CD9 in the adhesion mediated by a variety of endothelial receptors (including vascular cell adhesion molecule [VCAM]-1 and ICAM-1) during leukocyte extravasation, a key event in the inflammatory response (7,19). This role suggests that localized release of blocking antibodies against CD9 might have potential as a general and more effective anti-inflammatory therapy than the single inhibition of one of these adhesion molecules. However, CD9 is not only expressed by endothelial cells but also by a number of blood cell subsets (including platelets, neutrophils, and monocytes) (7,20). Therefore, the administration of CD9 blockers would require a localized release in inflammatory foci, which could be accomplished by their combination with antibodies against any inflammatory marker in the same MB.

Inflammation is a crucial component of many cardiovascular disorders from the earliest stages, and the potential of MB to identify sites of inflammation is therefore of great interest. In small animal models, inflammation can be visualized and quantified by introducing MB targeted to several well-established biomarkers such as P-selectin (21) or VCAM-1 (22). Here, we have developed an ex vivo model of inflammation in human macrovasculature by using ICAM-1 as an inflammatory marker. We found that ICAM-1 is expressed at basal levels in resting endothelium, but this basal expression seems to be below the detection threshold of our imaging technique. Therefore, the anti–ICAM-1–tagged MB specifically highlighted the endothelium of vessels exposed to proinflammatory stimuli, validating this approach as a means of detecting inflammatory foci in large vessels.

The use of MB in combination with US has been shown to promote gene delivery in a variety of experimental animal models (reviewed in Miller et al. [23]). Our ex vivo experiments in human umbilical cord vessels show that sonoporation is practicable in the human vasculature. However, the transfection efficiency was limited by the fact that the cells in the ex vivo model remain in a quiescent-like state, with low metabolic activity, which precludes a high protein yield from the transfected plasmid. Moreover, our experiments were performed with nontagged MB mixed with DNA in solution. The development of MB able to couple both antibodies and DNA at their outer surface might be critical for improving the

efficiency of targeted sonoporation. It should also be noted that the sensitivity of our detection technique is lower than bioluminescence, for example. Nevertheless, our findings demonstrate the potential application of sonoporation in human tissue and thus constitute an important step toward the therapeutic use of noninvasive methods for gene therapy.

CONCLUSIONS

The human umbilical cord is a feasible ex vivo model for the study and development of therapeutic MB applications and also constitutes a unique and irreplaceable system to test for the functional specificity of antihuman antibodies. However, there are several limitations that cannot be overlooked, such as the fact that this model is a simplified ex-sanguine one in which the absence of blood cells and lack of physiologic flow could affect the binding of MB, and the requirement for humanized antibodies, peptides, or plasmids tested and approved by the Food and Drug Administration for clinical administration.

Acknowledgments

The authors thank Dr. Pilar Martín and Marta Ramírez for technical assistance, and Simon Barlett for critical reading of the manuscript.

Reprint requests and correspondence: Dr. Francisco Sánchez-Madrid, Servicio de Inmunología, Hospital de la Princesa, Universidad Autónoma de Madrid, C/ Diego de León 62, 28006 Madrid, Spain. *E-mail: fsanchez.hlpr@salud.madrid.org.*

REFERENCES

1. Dayton PA, Rychak JJ. Molecular ultrasound imaging using microbubble contrast agents. Front Biosci 2007;12:5124–42.
2. Deng CX, Sieling F, Pan H, Cui J. Ultrasound-induced cell membrane porosity. Ultrasound Med Biol 2004;30:519–26.
3. Tachibana K, Tachibana S. The use of ultrasound for drug delivery. Echocardiography 2001;18:323–8.
4. Meijering BD, Henning RH, Van Gilst WH, Gavrilovic I, Van Wamel A, Deelman LE. Optimization of ultrasound and microbubbles targeted gene delivery to cultured primary endothelial cells. J Drug Target 2007;15:664–71.
5. Villanueva FS, Jankowski RJ, Klibanov S, et al. Microbubbles targeted to intercellular adhesion molecule-1 bind to activated coronary artery endothelial cells. Circulation 1998;98:1–5.
6. Barreiro O, Yanez-Mo M, Serrador JM, et al. Dynamic interaction of VCAM-1 and ICAM-1 with moesin and ezrin in a novel endothelial docking structure for adherent leukocytes. J Cell Biol 2002;157:1233–45.
7. Barreiro O, Yanez-Mo M, Sala-Valdes M, et al. Endothelial tetraspanin microdomains regulate leukocyte firm adhesion during extravasation. Blood 2005;105:2852–61.
8. Christiansen JP, Leong-Poi H, Klibanov AL, Kaul S, Lindner JR. Noninvasive imaging of myocardial reperfusion injury using leukocyte-targeted contrast echocardiography. Circulation 2002;105:1764–7.
9. Weller GE, Lu E, Csikari MM, et al. Ultrasound imaging of acute cardiac transplant rejection with microbubbles targeted to intercellular adhesion molecule-1. Circulation 2003;108:218–24.
10. Lanza GM, Wallace KD, Scott MJ, et al. A novel site-targeted ultrasonic contrast agent with broad biomedical application. Circulation 1996;94:3334–40.
11. Rychak JJ, Klibanov AL, Ley KF, Hossack JA. Enhanced targeting of ultrasound contrast agents using acoustic radiation force. Ultrasound Med Biol 2007;33:1132–9.
12. Tsutsui JM, Xie F, Cano M, et al. Detection of retained microbubbles in carotid arteries with real-time low mechanical index imaging in the setting of endothelial dysfunction. J Am Coll Cardiol 2004;44:1036–46.
13. Lindner JR. Detection of inflamed plaques with contrast ultrasound. Am J Cardiol 2002;90:32L–5L.
14. Weller GE, Wong MK, Modzelewski RA, et al. Ultrasonic imaging of tumor angiogenesis using contrast microbubbles targeted via the tumor-binding peptide arginine-arginine-leucine. Cancer Res 2005;65:533–9.
15. Schumann PA, Christiansen JP, Quigley RM, et al. Targeted-microbubble binding selectively to GPIIb IIIa receptors of platelet thrombi. Invest Radiol 2002;37:587–93.
16. Gutierrez-Lopez MD, Ovalle S, Yanez-Mo M, et al. A functionally relevant conformational epitope on the CD9 tetraspanin depends on the association with activated beta1 integrin. J Biol Chem 2003;278:208–18.
17. Erovic BM, Neuchrist C, Kandutsch S, Woegerbauer M, Pammer J. CD9 expression on lymphatic vessels in head and neck mucosa. Mod Pathol 2003;16:1028–34.
18. Hemler ME. Tetraspanin functions and associated microdomains. Nat Rev Mol Cell Biol 2005;6:801–11.
19. Barreiro O, Zamai M, Yanez-Mo M, et al. Endothelial adhesion receptors are recruited to adherent leukocytes by inclusion in preformed tetraspanin nanoplatforms. J Cell Biol 2008;183:527–42.
20. Tohami T, Drucker L, Radnay J, Shapira H, Lishner M. Expression of tetraspanins in peripheral blood leukocytes: a comparison between normal and infectious conditions. Tissue Antigens 2004;64:235–42.
21. Lindner JR, Song J, Christiansen J, Klibanov AL, Xu F, Ley K. Ultrasound assessment of inflammation and renal tissue injury with microbubbles targeted to P-selectin. Circulation 2001;104:2107–12.
22. Kaufmann BA, Sanders JM, Davis C, et al. Molecular imaging of inflammation in atherosclerosis with targeted ultrasound detection of vascular cell adhesion molecule-1. Circulation 2007;116:276–84.
23. Miller DL, Pislaru SV, Greenleaf JE. Sonoporation: mechanical DNA delivery by ultrasonic cavitation. Somat Cell Mol Genet 2002;27:115–34.

Key Words: ultrasound ■ microbubbles ■ human umbilical cord ■ targeting ■ inflammation ■ sonoporation.

▶APPENDIX

For an expanded Methods section, please see the online version of this article.